

EFFECTS OF CATIONIC SUBSTITUTIONS AND ALTERATION IN URANINITE, AND IMPLICATIONS FOR THE DATING OF URANIUM DEPOSITS

PAUL ALEXANDRE[§] AND T. KURT KYSER

Department of Geological Sciences and Geological Engineering, Queen's University, Kingston, Ontario K7L 3N6, Canada

ABSTRACT

Uraninite grains from two sites of unconformity-type uranium mineralization, the high-grade basement-hosted McArthur River deposit and the sediment-hosted Virgin River prospect in the Paleoproterozoic Athabasca Basin in northern Saskatchewan, Canada, were investigated with a scanning electron microscope and analyzed with an electron microprobe. Electron back-scatter images, chemical compositions and calculated chemical U/Pb ages from the uraninite indicate substitution of radiogenic Pb by Ca, Si, and Fe from later fluid-circulation events after initial formation of the uraninite at *ca.* 1600 Ma. Conversion of uraninite to coffinite, with SiO₂ up to 10 wt%, seems to have occurred at *ca.* 700 Ma. The intensity and the character of the substitutions depend on both the amount and the composition of the alteration fluids, which may be influenced by the characteristics of the host rocks.

Keywords: uraninite, crystal chemistry, U–Pb chemical ages, Athabasca Basin, unconformity-type uranium deposits, Saskatchewan, Canada.

SOMMAIRE

Des grains d'uraninite provenant de deux zones de minéralisation en uranium de type discordance, le gisement à teneur élevée de McArthur River, situé dans le socle, et la minéralisation de Virgin River, située dans les grès, dans le bassin Paléoprotérozoïque d'Athabasca, Saskatchewan, Canada, ont été étudiés par microscope électronique à balayage et par microsonde électronique. L'imagerie en électrons rétrodiffusés, la composition chimique, et les âges chimiques U–Pb calculés pour l'uraninite indiquent un remplacement du plomb radiogénique par Ca, Si et Fe, au cours d'événements de circulation de fluide après la minéralisation initiale, survenue à environ 1600 Ma. La conversion de l'uraninite à la coffinite, avec près de 10% poids de SiO₂, est survenue vers 700 Ma. L'intensité et le caractère des substitutions dépendent de la quantité et la composition chimique de la phase fluide, qui pourrait avoir été influencée par les caractéristiques des roches encaissantes.

Mots-clés: gisements d'uranium de type discordance, uraninite, cristallographie, âges chimiques U–Pb, bassin d'Athabasca, Saskatchewan, Canada.

INTRODUCTION

Uraninite, UO₂ (Janeczek & Ewing 1992a), is the most common uranium-bearing mineral in unconformity-type uranium deposits. It can contain up to 90 wt% U, much more than other primary uranium minerals such as brannerite, davidite or coffinite. However, thorium, rare-earth elements (REE), calcium, and radiogenic elements such as lead, radium, and polonium may be encountered in natural uraninite, which makes its formula (U⁴⁺_{1-x-y-z} U⁶⁺_x REE³⁺_y M²⁺_z) O_{2+x-y-z} (Janeczek & Ewing 1992a, Finch & Murakami 1999). Uranium is transported as U⁶⁺, as various uranyl

complexes in oxidizing solutions, and precipitates under reducing conditions as U⁴⁺O₂ (Huré & Elston 1960, Brookins 1978).

Uraninite is a chemically active mineral and readily exchanges elements or recrystallizes during subsequent fluid-circulation events (Grandstaff 1976, Finch & Ewing 1992, Kotzer & Kyser 1993). Isobe *et al.* (1992), Janeczek & Ewing (1995) and Kempe (2003) have demonstrated in electron-microprobe studies that most natural uraninite is chemically heterogeneous at the micrometer scale. This characteristic results in analytical complications if uraninite is used for isotopic dating.

[§] *Current address:* SUERC, Technology Park, Rankine Avenue, East Kilbride, Glasgow G75 0QF, UK. *E-mail address:* p.alexandre@suerc.gla.ac.uk

The two major isotopes of uranium, ^{238}U and ^{235}U , decay to ^{206}Pb and ^{207}Pb , respectively, which leads to the presence of variable amounts of radiogenic lead in the structure of uraninite. As Pb^{2+} has a larger ionic radius (1.37 Å) than U^{4+} (1.05 Å) and a different valence, it is incompatible with the crystal structure. On the other hand, alteration of uraninite will form common uranium minerals such as coffinite $\text{U}(\text{SiO}_4)_{1-x}(\text{OH})_{4x}$, soddyite $(\text{UO}_2)_2\text{SiO}_4(\text{H}_2\text{O})_2$, uranophane $\text{Ca}[(\text{UO}_2)\text{SiO}_3(\text{OH})]_2(\text{H}_2\text{O})_5$, or becquerelite $\text{Ca}[(\text{UO}_2)_6\text{O}_4(\text{OH})_6](\text{H}_2\text{O})_8$ containing variable amounts of REE (ca. 1.06 Å), Ca (1.06 Å), and Si (Finch & Murakami 1999). Partial oxidation also occurs, leading to mixed oxidized-reduced uranium compounds such as $\text{U}^{5+}_2\text{U}^{4+}\text{O}_7$ or $\text{U}^{5+}_2\text{U}^{6+}\text{O}_8$ (Finch & Ewing 1992).

Here we report the element substitutions and effects of alteration and recrystallization in natural uraninite on the basis of electron-microprobe data and scanning electron microscopy (SEM) images. The samples studied are from unconformity-type uranium concentrations in the Athabasca Basin, northern Saskatchewan, Canada. The results provide a particularly good example of how post-mineralization fluid-circulation events affect and change the composition of uraninite over geological time.

GEOLOGY AND PETROGRAPHY

Two sets of samples representing two different geological settings were used for the present study. One set of samples comes from the high-grade ore zone at the McArthur River uranium deposit, and the other from the Virgin River exploration prospect (Fig. 1), both operated by the Cameco Corporation. Both are sites of unconformity-type uranium mineralization. The samples from McArthur River are representative of a basement-hosted orebody (McGill *et al.* 1993), whereas the mineralization at Virgin River is entirely sandstone-hosted.

General geology

The basement of the Athabasca Basin is composed of Archean and Aphebian rocks that were metamorphosed during the Hudsonian Orogeny (Lewry & Sibbald 1980). They are part of the Wollaston Domain in the Cree Lake mobile zone, itself situated between the Western craton and the Trans-Hudson Orogen (Lewry & Sibbald 1980; Fig. 1). The Wollaston Domain comprises mainly Archean and Paleoproterozoic continental crust and supracrustal rocks representative of a continental

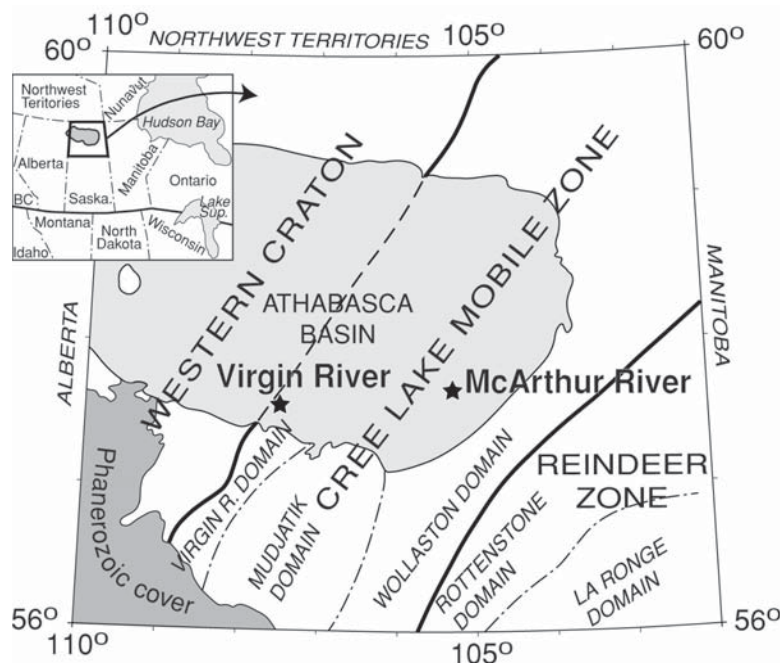


Fig. 1. Simplified geological map of the Paleoproterozoic Athabasca Basin, showing the location of the basement-hosted McArthur River deposit and the sandstone-hosted Virgin River prospect. Modified from Hoeve & Sibbald (1978) and Sibbald & Quirt (1987).

margin (Hoeve & Sibbald 1978). Four main groups of rocks are distinguished in the basement complex (Lewry & Sibbald 1980): (i) Archean orthogneisses and subordinate metamorphic rocks, (ii) high-grade metasedimentary units of the Wollaston Group, (iii) deformed calc-alkaline granitic rocks and minor gabbros, and (iv) peraluminous granitic rocks of various types. Calc-silicate rocks and dolomites represent some of the minor units (Sibbald & Quirt 1987).

The Athabasca Basin formed at *ca.* 1730 Ma (Kyser *et al.* 2000). The basin fill consists of thick clastic sequences of Paleoproterozoic age (Ramaekers 1990) resulting from the rapid exhumation of the Trans-Hudson Orogen (Kyser *et al.* 2000). The basin is subdivided into three sub-basins, with most of the uranium deposits, including the McArthur River deposit, found in the easternmost, Cree sub-basin. Sedimentary rocks of the lowermost Manitou Falls Formation of the Athabasca Group host most of the deposits in this area; this formation is subdivided into three members: (i) a basal series of interbedded conglomerates and sandstones, (ii) a middle clean sandstone, and (iii) an upper clay- and intraclast-rich member (Ramaekers 1990).

The McArthur River orebody

The central part of the basement-hosted uranium orebody from which the samples were taken consists of massive uraninite (McGill *et al.* 1993). A distal illite-bearing zone of alteration and a proximal chlorite-bearing zone of alteration surround it, and the latter formed after the former. Mineralization is a result of precipitation of uranium minerals from basinal fluids evolved from seawater, when they penetrated the reducing basement along fractures related to the major NNE–SSW-oriented zone of reverse faults (McGill *et al.* 1993, Fayek & Kyser 1997). The age of the initial precipitation of uranium minerals is fixed between the $^{40}\text{Ar}/^{39}\text{Ar}$ age of 1591 ± 21 Ma for syn-ore illite and the $^{207}\text{Pb}/^{206}\text{Pb}$ age of 1570 ± 19 Ma for uraninite (Alexandre *et al.* 2004).

The Virgin River prospect

This prospect is situated in the central-west part of the Athabasca Basin (Fig. 1), and is hosted by the Manitou Falls Formation of the Athabasca Group. Uranium mineralization is represented by disseminated uraninite in sandstones, with uraninite grains rarely exceeding 150 μm across. Strong alteration to kaolinite and illite surrounds the mineralized zones, as well as small amounts of chlorite and spherulitic dravite. The age of uranium mineralization at the Virgin River prospect is *ca.* 1590 Ma, as determined by U/Pb and $^{207}\text{Pb}/^{206}\text{Pb}$ dating of uraninite (Alexandre *et al.* 2004).

ANALYTICAL PROCEDURE

Electron-microprobe procedure

Polished thin sections were examined with reflected-light optical microscopy and scanning electron microscopy (SEM). We used a JEOL 6400 digital scanning electron microscope equipped with a Link Systems energy-dispersion spectrometer (EDX) at Carleton University, Ottawa, Canada. Photographs were taken of the areas to be investigated, thus facilitating placement of the beam for electron-microprobe analyses. Quantitative analyses using polished thin sections were performed at Carleton University, on an automated four-spectrometer Camebax MBX electron microprobe with wavelength-dispersion spectrometry (WDX). Operating conditions were: 15 kV accelerating potential, 20 nA beam current for silicates and oxides. Peaks were counted between 15 and 40 seconds; the background on each side of the analyzed peak was counted for half that time. Wavelength scans were made near the peak position of each element sought to check for interferences and to choose optimum (interference-free) background positions. Raw X-ray data were converted to elemental weight % with the Cameca PAP matrix-correction program. A suite of well-characterized minerals and synthetic compounds were used as standards. Analytical results are considered accurate to 1–2% relative for major elements, 3–5% relative for minor elements (<1 wt%). We sought the elements Si, Ca, Fe, Ti, Pb, and U.

X-ray diffraction

The X-ray diffraction (XRD) analyses were performed on selected thin sections containing massive uraninite, using a Philips X'Pert[®] instrument with a sample holder and source optimized for thin section analyses. We used $\text{CuK}\alpha$ radiation ($\lambda = 1.5406 \text{ \AA}$), and the X'Celerator[®] detector in scanning mode. We scanned from 5 to $85^\circ 2\theta$, which covers all major peaks of uraninite. A long counting-time of 20 seconds per step was used in order to improve counting statistics.

Calculations of age

There are several methods for age calculation on the basis of the chemical composition of uranium-rich minerals, or chemical ages (Bowles 1990). They are all based on the assumption that all lead contained in the analyzed mineral, uraninite in this case, is radiogenic, and that uranium has not been re-introduced into the system.

We used the iteration of the formula $^{206}\text{Pb}/^{238}\text{U} = \exp(\lambda_{238}t) - 1$, as suggested by Bowles (1990). This

calculation is based on the supposition that the proportion of radiogenic lead coming from thorium is negligible, as thorium is but a minor component of uraninite in a sedimentary environment (Janeczek & Ewing 1992b; it is below the detection limit in our samples) and decays more slowly than uranium. The amount of ^{206}Pb was calculated using the total lead content (atom wt%), and the $^{206}\text{Pb}/^{207}\text{Pb}$ ratio was calculated from the age of the previous iteration (1000 Ma for the first iteration). The amount of ^{238}U was calculated from the total uranium content (atom wt%) and the $^{238}\text{U}/^{235}\text{U}$ value of uranium in nature. Only four iterations were needed to calculate an age with precision to the second decimal point. Our calculations give ages slightly higher (*ca.* 10 Ma in our case, *i.e.*, less than 1%) than the empirical formula of Ranchin (1968), which is best adapted for ages less than 200 Ma.

OPTICAL MICROSCOPY AND SCANNING ELECTRON MICROSCOPY OF URANINITE

The McArthur River deposit

Reflected-light microscopy (Fig. 2) shows that the uraninite from the basement-hosted McArthur River deposit commonly is euhedral (sample 230–528) or colloform (sample 198–555.2A). Many samples display a homogeneous reflectance, such as sample 230–528 (Fig. 2), but in most cases the uraninite crystals have zones of different reflectivity, as observed in samples 198–555.2C and 204–507.8A (Fig. 2), or porous zones, as in sample 198–555.2 B (Fig. 2). The zones of lower reflectivity in the samples correspond to altered and recrystallized uraninite under reducing conditions (mostly conversion to coffinite) or under oxidizing conditions, leading to formation of uranyl oxyhydroxydes (Finch & Murakami 1999). These darker zones are seen either along the edge of the grain (*e.g.*, 204–207.8A) or along fractures within the grain (*e.g.*, 204–507.8B).

Zones that appear to be homogeneous in reflected light (Fig. 3A) commonly reveal the presence of areas with variable brightness when observed by SEM (Fig. 3B). The brightness variation in back-scattered electron (BSE) images is characteristic of different chemical compositions because it is a function of the average atomic weight. These areas have irregular shapes, independent of the morphology of the grain, and vary in size from a few to nearly 100 μm (Fig. 3B).

The Virgin River prospect

Although the dispersed and irregularly shaped grains of uraninite of the sandstone-hosted Virgin River prospect invariably seem to be homogeneous in reflected light (Fig. 4A), they show zones of variable brightness in SEM (Fig. 4B). It is noticeable that the brighter areas, corresponding to higher average atomic weight

and therefore to higher uranium content, are relatively limited ($\leq 10 \mu\text{m}$) and that most of the grain is darker, corresponding to altered uraninite (Finch & Murakami 1999). Such darker areas probably indicate a higher degree of alteration or recrystallization of the uraninite at the Virgin River prospect, relative to McArthur River uraninite.

The comparison between reflected-light images and the SEM images indicates that heterogeneity can be observed by both methods, even though in many cases it is not visible by optical microscopy. This heterogeneity corresponds to the chemical variability of the uraninite and is due to alteration or recrystallization, as observed by Finch & Murakami (1999) and Fayek *et al.* (2002).

X-RAY-DIFFRACTION RESULTS

The analyses by X-ray diffraction (XRD) show that the major mineral of uranium is uraninite, accounting for up to 98% of the volume. Small but distinct peaks corresponding to coffinite are visible at 4.19, 3.50, 2.47, and 1.87 \AA (angles of 21.2, 25.4, 36.4, and $48.6^\circ 2\theta$). Still weaker and less well-defined peaks, some of them difficult to distinguish from the background, probably correspond to trace amounts of a variety of uranium hydroxides and hydrous silicates, including becquerelite, haiweeite, schoepite, and curite, containing various quantities of calcium, sodium, lead, and carbon. These minerals and the coffinite are alteration products of uraninite, on the basis of the petrographic and SEM results.

CHEMICAL COMPOSITION OF URANINITE

The McArthur River deposit

The concentration of uranium in uraninite from the McArthur River deposit is quite variable, with UO_2 from 71.38 to 83.84 wt% (Table 1). All other elements also vary significantly; the Pb content varies from 1.86 to 16.71 wt% PbO, Si, from 0.03 to 9.66 wt% SiO_2 , Fe, from 0.10 to 1.84 wt% FeO, and Ca, from 0.06 to 3.45 wt% CaO. Only Ti is relatively constant, ranging from 0.13 to 0.76 wt% TiO_2 (Table 1).

The data define two groups of uraninite, with one representing the majority of the uraninite and having high lead and low uranium, silicon, calcium, and iron contents. The other group has low lead and high uranium, silicon, calcium, and iron contents (Table 1, Fig. 5A). The average concentrations of elements in the two groups are significantly different. The average contents of U are 81.40 ± 1.02 and 73.48 ± 1.63 wt% UO_2 , of Pb, 14.18 ± 1.80 and 3.30 ± 1.98 wt% PbO, of Si, 0.18 ± 0.11 and 8.84 ± 0.88 wt% SiO_2 , of Fe, 0.28 ± 0.15 and 1.61 ± 0.18 wt% FeO, and Ca, 1.00 ± 0.29 and 3.26 ± 0.21 wt% CaO, respectively. The group with high Pb contents and low concentrations of Si,

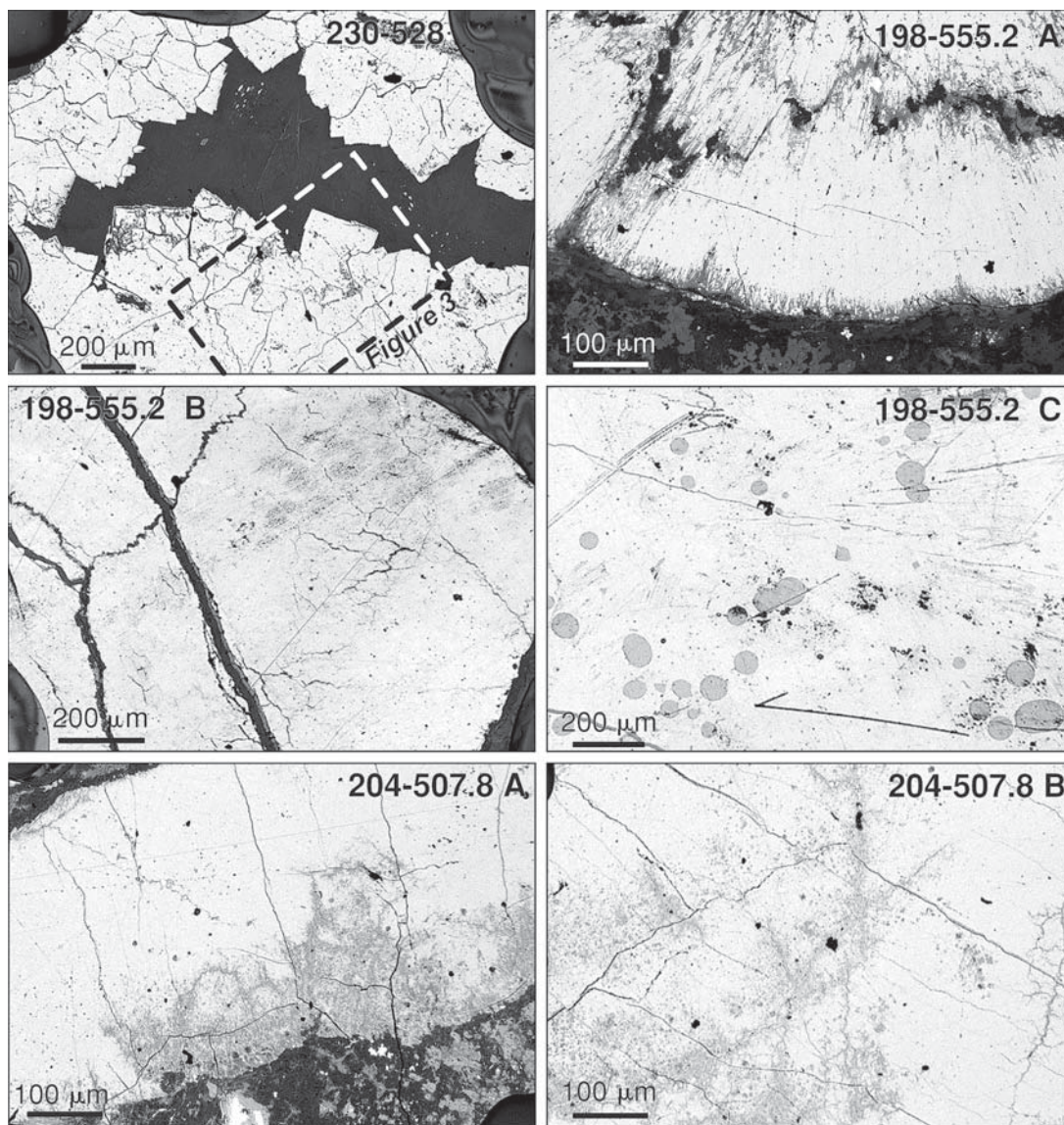


FIG. 2. Reflected-light photomicrographs illustrating the variety of morphology and texture in uraninite from the massive uraninite ore-zone of the basement-hosted McArthur River deposit. Uraninite can be apparently completely homogeneous, as with sample 230-528. All other samples display various degrees of alteration (lower-reflectivity areas) at the edge of grains (samples 198-555.2A and 204-507.8A) or along fractures (sample 204-507.8B). Sample 198-555.2C displays globular zones with sharp edges, corresponding to recrystallized uraninite. Sample 198-555.2B displays round porous zones, corresponding either to defects in the structure of uraninite as result of strong alteration, or to the accumulation of radiogenic ^4He (Finch & Murakami 1999). Two major morphologies are present, euhedral (sample 230-528) and colloform (samples 198-555.2A and 204-507.8A).

Ca, and Fe (Table 1) corresponds to variably altered uraninite (Janeczek & Ewing 1992b). The low-lead group corresponds to coffinite and possibly to minor uranium silicates and hydroxides such as soddyite and

uranophane, as the high concentrations of Si and Ca and the low totals suggest; we assume that the lower totals reflect the presence of structural H_2O . Titanium has similar concentrations in both groups, with average

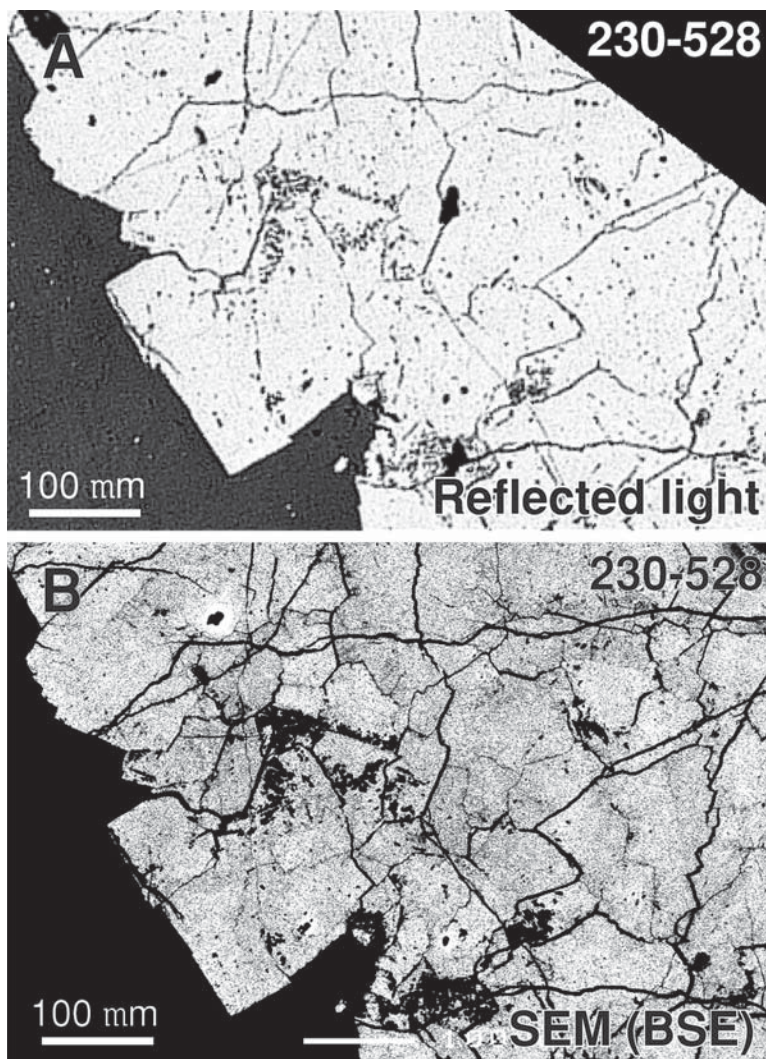


FIG. 3. Comparison between reflected-light microscopy (A) and scanning electron microscopy (SEM) in back-scattered-electron images (B) for sample 230-528 from McArthur River. Whereas the reflected-light image shows a completely homogeneous mineral, the SEM image indicates a subtle heterogeneity in the distribution of mean atomic weight, consistent with differences in chemical composition on the micrometer scale.

TiO₂ of 0.35 ± 0.17 and 0.45 ± 0.06 wt%, respectively. Finally, two groups of uraninite can be distinguished on the basis of their Fe content (Fig. 5B).

A statistical treatment of the chemical composition of the uraninite samples analyzed, such as a correlation matrix (Table 2) and factorial analysis (Fig. 6), brings out correlations among various elements, corresponding to the mineralogy of the uranium phases present. The most significant anticorrelation observed is between uranium and lead (Fig. 6), with a Spearman rank corre-

lation coefficient of -0.89 (Table 2), which results from the radioactive disintegration of uranium producing lead. Uranium, iron, and calcium have strongly negative F1 values (Fig. 6), and are grouped in the factorial analysis diagram (Fig. 6), indicating that they are correlated. This is confirmed by their positive Spearman rank correlation coefficients, from 0.51 to 0.58 (Table 2). This group is anticorrelated with Pb (Fig. 6), which is consistent with uraninite alteration leading to Pb loss and concomitant integration of Ca and Fe. Titanium is

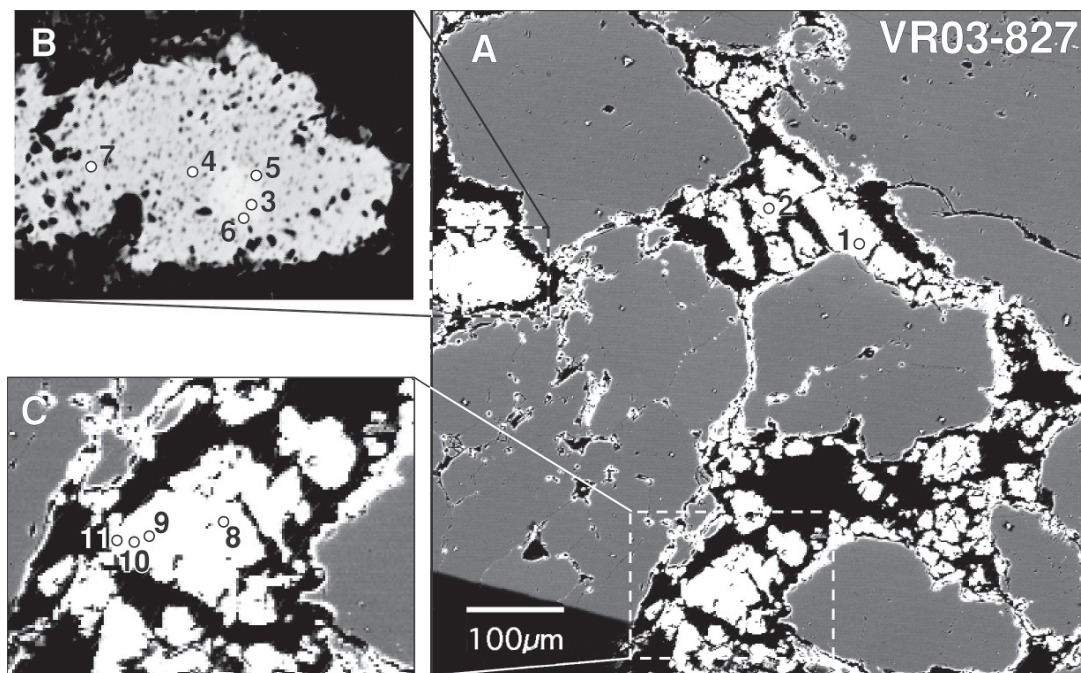


FIG. 4. Reflected-light photomicrograph (A, C) and SEM image (B) of disseminated grains of uraninite (white) in sandstone host-rock (grey) from Virgin River. The position of the spots analyzed with the electron microprobe (Table 1) are shown. Note the heterogeneity in a grain (B).

not correlated with any other element, probably because it is present as a discrete TiO_2 phase such as anatase.

The Virgin River prospect

The concentration of uranium in sandstone-hosted uraninite at Virgin River is variable, with UO_2 varying from 79.04 to 83.28 wt% (Table 3). The concentration of silicon is relatively constant (from 0.24 to 0.40 wt% SiO_2), as are Ca (from 1.16 to 1.91 wt% CaO) and Ti (from 0.20 to 0.30 wt% TiO_2 ; Table 3). Variability in Fe content is greater, from 0.86 to 4.07 wt% FeO (Table 3). Lead concentrations are low, ranging from 0.18 to 0.61 wt% PbO. The low lead contents can be attributed to severe loss of lead during alteration of the uraninite. Three analyses of uraninite from Virgin River have abnormally high iron contents (FeO from 1.78 to 4.07 wt%; Fig. 7), distinct from the anticorrelation trend between $\text{SiO}_2 + \text{CaO} + \text{FeO}$ and PbO contents observed for all other samples analyzed (Fig. 7A).

A compositional profile consisting of four analyses was obtained for one grain (Fig. 4C). The results indicate that iron content increases toward the edge of the grain, whereas lead content decreases (Fig. 7B). Calcium content also increases toward the edge of the grain, although it decreases at the very edge. Silicon and

titanium contents are relatively invariant. The profiles of iron and calcium are consistent with diffusion of these elements into the grain, whereas the profile of lead indicates diffusion out of the grain. This finding illustrates that lead loss and iron and calcium gain are related, corresponding to the replacement of the former by the latter in the structure.

CATION SUBSTITUTIONS IN URANINITE

Uraninite from the basement-hosted McArthur River deposit displays a negative correlation between PbO and $\text{SiO}_2 + \text{CaO} + \text{FeO}$ contents (Fig. 5), consistent with Pb loss being commensurate with gain in Si, Ca and Fe. The distribution of the calculated chemical ages for uraninite from the McArthur River deposit (Fig. 8) shows the dominance of four ages at 1217 ± 29 , 1113 ± 27 , 910 ± 22 , and 682 ± 19 Ma. These ages correspond to dominant $^{40}\text{Ar}/^{39}\text{Ar}$ ages of associated clay minerals and U–Pb ages of uraninite from the basement-hosted McArthur River deposit and from two sediment-hosted prospects in the west part of the Athabasca Basin (Alexandre *et al.* 2005). A grouping of ages, rather than a random distribution, indicates that substitution of elements occurred preferentially during distinct periods of fluid flow. These periods correspond

to emplacement of mafic dykes in the Athabasca Basin at *ca.* 1270 Ma (Burwash *et al.* 1962, Le Cheminant & Heaman 1989) and far-field tectonic events, corresponding to the Grenvillian Orogeny at *ca.* 1100 Ma (Moore 1986) and the initial break-up of Rodinia at *ca.* 900 Ma (Kyser *et al.* 2000). Similar substitutions in uraninite at particular periods have been observed by Fayek *et al.* (1997), who analyzed sandstone-hosted uraninite, and attributed distinct compositional groups to various stages of uranium mineralization characterized by distinct minerals of uranium. That the cation substitutions in uraninite occur at particular times is to be expected, as it is a direct consequence of the enhanced circulation of fluid at these times. Indeed, the initial stage of mineralization occurred at 1590 Ma (Alexandre *et al.* 2005) and is itself the product of fluid circulation related to the initial stages of the Mazatzal Orogeny (Romano *et al.* 2000, Medaris *et al.* 2003). Given that cation substitutions appear to reflect alteration of pre-existing uraninite rather than addition of uranium from the alteration fluids, the majority of the uraninite samples from McArthur River belong to the same initial stage of mineralization that was modified

by subsequent fluid-circulation events, which in turn underlines the importance of fluid-circulation evolution for uranium mineralization and its preservation.

Calcium is the most common element to replace uranium in the structure of uraninite. This is because calcium has the ionic radius closest to that of uranium (1.06 Å and 1.05 Å, respectively). Lead, with its ionic radius of 1.37 Å, is rapidly displaced from the uraninite crystal. The two other substituting elements, Si and Fe, have significantly smaller ionic radii, and presumably cannot replace Pb in uraninite, but form discrete uranium-bearing alteration phases, such as coffinite.

The four compositions with much higher contents of Si at the McArthur River deposit (SiO₂ up to 9.7 wt%; Table 1) reflect a conversion of uraninite to coffinite under reducing conditions, a common occurrence in natural uraninite (Janeczek & Ewing 1992b). Although the stability of uraninite relative to coffinite during the initial precipitation of uraninite from uranium-bearing fluids is not well understood (Finch & Murakami 1999), it is possible that the conversion of uraninite to coffinite corresponds to increased amount of dissolved silica in more reduced fluids.

TABLE 1. RESULTS OF ELECTRON-MICROPROBE ANALYSES AND CALCULATED CHEMICAL U-Pb AGES FOR URANINITE AND COFFINITE (SHADED) FROM THE McARTHUR RIVER BASEMENT-HOSTED URANIUM DEPOSIT, ATHABASCA BASIN

	SiO ₂	PbO	UO ₂	FeO	CaO	TiO ₂	Total	Age		SiO ₂	PbO	UO ₂	FeO	CaO	TiO ₂	Total	Age
230-528, A1	0.21	14.73	81.40	0.22	0.88	0.25	97.69	1113	198-555.2, C-5	0.20	14.03	81.44	0.23	0.97	0.52	97.38	1065
230-528, A2	0.11	16.31	80.19	0.15	0.67	0.21	97.63	1233	198-555.2, C-6	0.35	13.09	82.21	0.38	1.09	0.60	97.72	992
230-528, A3	0.37	12.47	82.94	0.29	1.02	0.47	97.56	943	198-555.2, C-7	0.17	14.81	80.19	0.15	0.79	0.42	96.54	1133
230-528, A4	0.23	13.62	81.81	0.34	0.76	0.44	97.20	1033	198-555.2, C-8	0.15	13.45	82.20	0.22	0.71	0.38	97.11	1017
230-528, A5	0.07	15.94	80.23	0.14	0.68	0.15	97.21	1208	198-555.2, C-9	0.14	14.12	81.77	0.22	0.75	0.33	97.32	1067
230-528, A6	0.11	16.44	80.47	0.12	0.78	0.22	98.15	1238	198-555.2, C-10	0.21	12.03	82.96	0.33	1.21	0.41	97.15	912
230-528, A7	0.25	13.24	82.34	0.27	1.07	0.33	97.51	1002	198-555.2, C-11	0.10	12.32	83.19	0.23	1.00	0.25	97.09	930
230-528, A8	0.39	12.76	83.21	0.37	1.26	0.45	98.44	959	198-555.2, C-12	0.14	14.15	81.98	0.12	0.81	0.29	97.48	1067
230-528, A9	0.23	13.60	81.89	0.23	0.90	0.45	97.30	1030	198-555.2, C-13	0.14	14.34	80.89	0.21	0.93	0.29	96.79	1093
230-528, A10	0.23	16.71	80.05	0.17	0.81	0.28	98.24	1261	198-555.2, C-14	0.08	15.66	80.86	0.14	0.59	0.37	97.71	1181
198-555.2, A-1	0.24	16.27	79.67	0.15	0.87	0.59	97.79	1237	198-555.2, C-15	0.14	14.72	81.61	0.16	0.77	0.45	97.85	1109
198-555.2, A-2	0.16	15.32	80.60	0.19	0.97	0.67	97.92	1162	198-555.2, C-16	0.11	15.26	80.84	0.15	0.89	0.36	97.60	1155
198-555.2, A-3	7.90	6.11	73.07	1.64	3.16	0.49	92.37	547	198-555.2, C-17	0.04	15.80	80.88	0.17	0.96	0.33	98.18	1190
198-555.2, A-4	0.24	15.05	80.66	0.32	0.82	0.67	97.75	1143	198-555.2, C-18	0.10	16.23	80.73	0.16	0.98	0.31	98.52	1220
198-555.2, A-5	9.50	1.98	74.34	1.84	3.45	0.42	91.53	181	198-555.2, C-19	0.08	15.84	80.37	0.18	0.89	0.31	97.68	1200
198-555.2, A-6	0.30	14.99	80.13	0.49	0.84	0.73	97.48	1145	198-555.2, C-20	0.06	14.61	81.47	0.18	0.71	0.31	97.34	1104
198-555.2, A-7	9.66	1.86	71.38	1.55	3.41	0.38	88.24	177	198-555.2, C-21	0.04	16.45	80.44	0.12	0.63	0.32	98.00	1239
198-555.2, A-8	8.28	3.24	75.12	1.41	3.02	0.50	91.58	290	204-507.8, A-1	0.09	14.83	80.76	0.38	1.07	0.13	97.26	1127
198-555.2, A-9	0.22	16.33	80.21	0.23	0.75	0.64	98.39	1234	204-507.8, A-3	0.10	15.78	80.00	0.16	0.84	0.15	97.04	1201
198-555.2, A-10	0.33	13.14	82.17	0.29	1.18	0.76	97.86	996	204-507.8, A-4	0.03	16.20	80.41	0.21	0.95	0.13	97.92	1223
198-555.2, A-11	0.13	15.84	80.31	0.18	0.76	0.71	97.92	1200	204-507.8, A-5	0.10	16.21	80.03	0.30	0.92	0.19	97.75	1229
198-555.2, B-1	0.29	11.84	81.36	0.32	1.51	0.37	95.68	915	204-507.8, A-6	0.16	12.24	82.12	0.57	1.34	0.20	96.62	935
198-555.2, B-2	0.46	9.56	83.84	0.45	2.07	0.28	96.66	731	204-507.8, A-7	0.16	13.79	81.32	0.50	1.16	0.13	97.07	1050
198-555.2, B-3	0.22	12.00	82.66	0.34	1.43	0.26	96.91	913	204-507.8, A-8	0.17	12.62	81.76	0.52	1.26	0.10	96.43	965
198-555.2, B-4	0.21	10.26	82.44	0.34	1.35	0.25	94.87	793	204-507.8, A-9	0.14	13.72	81.68	0.49	1.00	0.18	97.20	1041
198-555.2, B-5	0.59	9.14	83.28	0.47	1.99	0.49	95.95	706	204-507.8, A-10	0.10	11.37	82.55	0.86	1.40	0.14	96.42	871
198-555.2, B-6	0.15	11.06	83.73	0.38	1.20	0.22	96.74	838	204-507.8, A-11	0.06	15.83	81.30	0.32	0.85	0.26	98.61	1187
198-555.2, B-7	0.15	12.95	81.78	0.27	1.13	0.22	96.50	987	204-507.8, A-12	0.16	12.55	81.97	0.72	1.26	0.13	96.79	958
198-555.2, B-8	0.18	14.21	81.16	0.21	1.18	0.13	97.08	1081	204-507.8, A-13	0.11	14.92	80.73	0.34	1.06	0.18	97.34	1133
198-555.2, B-9	0.21	14.69	81.11	0.21	1.10	0.56	97.88	1114	Average	0.18	14.18	81.40	0.28	1.00	0.35	97.37	
198-555.2, B-10	0.15	14.27	81.18	0.17	1.02	0.21	97.01	1084	± 1σ	0.11	1.80	1.02	0.15	0.29	0.17	0.71	
198-555.2, C-1	0.14	15.02	81.39	0.10	0.79	0.45	97.89	1132	Average	8.84	3.30	73.48	1.61	3.26	0.45	90.93	
198-555.2, C-2	0.07	15.60	81.72	0.11	0.87	0.33	98.70	1166	± 1σ	0.88	1.98	1.63	0.18	0.21	0.06	1.84	
198-555.2, C-3	0.16	14.70	81.35	0.12	0.78	0.40	97.50	1111									
198-555.2, C-4	0.07	15.72	80.11	0.15	0.75	0.39	97.19	1195									

The compositions are reported in wt%, and the age, in Ma.

The alteration of uraninite under oxidizing conditions is relatively restricted at the McArthur River deposit, because the analytical totals are commonly

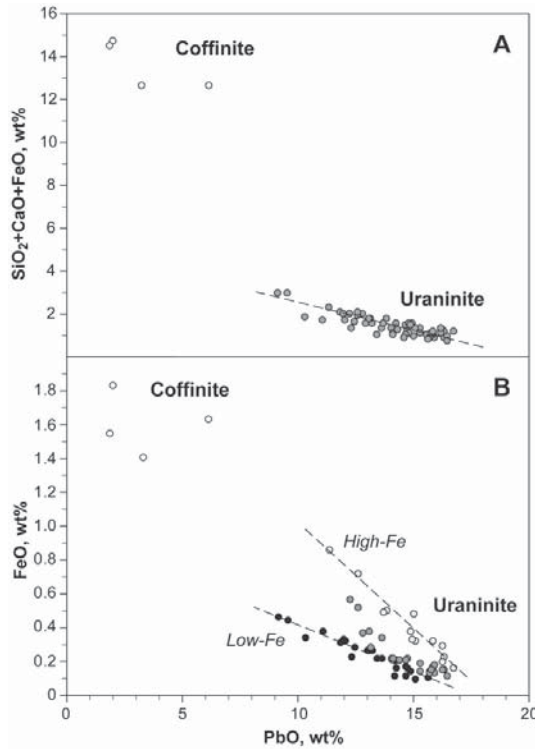


FIG. 5. Compositional variation of uraninite from the basement-hosted McArthur River deposit, showing negative correlation between $\text{SiO}_2 + \text{CaO} + \text{FeO}$ and PbO (A) and between FeO and PbO (B). The composition of coffinite (white circles) is distinct (A). The negative correlation between FeO and PbO contents (B) can be divided into high-iron (light grey circles) and low-iron trends (black circles).

relatively high (95 to 99 wt%; Table 1), whereas it is more significant at the Virgin River prospect (totals of 87 to 92 wt%; Table 3). The higher degree of alteration of uraninite at the Virgin River prospect relative to that at the McArthur River deposit, as indicated by the much lower Pb contents and the lower totals for the Virgin River uraninite (*cf.* Tables 1, 3), is also reflected by the much lower U–Pb chemical ages at Virgin River. These range from 14.5 to 53.2 Ma (Table 3), and have no meaning in terms of age of mineralization, when compared with the *ca.* 1590 Ma obtained by U–Pb LA–ICP–MS dating (Alexandre *et al.* 2004). These results emphasize the very strong and long-lasting alteration of uraninite at Virgin River. This stronger

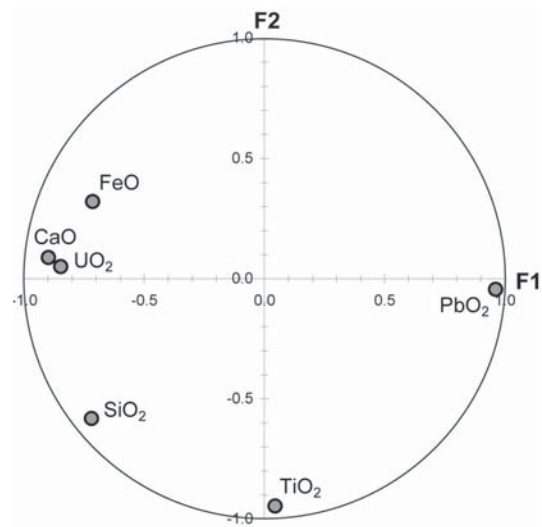


FIG. 6. Factorial analyses of the chemical compositions of uraninite from McArthur River, shown in the factor-plot space of the two first factors. Calcium and U are strongly correlated (F1 of -0.90 and -0.85 , respectively) and are anticorrelated with Pb (F1 of 0.96). Ti is independent.

TABLE 2. CORRELATION DIAGRAM FOR THE ANALYZED URANINITE FROM THE BASEMENT-HOSTED McARTHUR RIVER DEPOSIT, ATHABASCA BASIN

	UO_2	PbO	SiO_2	FeO	CaO	TiO_2
UO_2	1					
PbO	<i>-0.89</i> / <i>-0.82</i>	1				
SiO_2	<i>0.39</i> / <i>0.50</i>	<i>-0.52</i> / <i>-0.62</i>	1			
FeO	<i>0.51</i> / <i>0.46</i>	<i>-0.67</i> / <i>0.62</i>	<i>0.46</i> / <i>0.32</i>	1		
CaO	<i>0.58</i> / <i>0.65</i>	<i>-0.72</i> / <i>0.82</i>	<i>0.44</i> / <i>0.63</i>	<i>0.70</i> / <i>0.62</i>	1	
TiO_2	<i>0.00</i> / <i>-0.07</i>	<i>0.05</i> / <i>0.08</i>	<i>0.45</i> / <i>0.44</i>	<i>-0.18</i> / <i>-0.21</i>	<i>-0.24</i> / <i>-0.14</i>	1

The Spearman Rank correlation is shown in bold, and the Pearson Product-Moment correlation is shown in italics. The major anticorrelations, such as UO_2 versus PbO , PbO versus SiO_2 , PbO versus CaO , and PbO versus FeO , are well visible in both correlation indices.

alteration reflects the difference in fluid flow between the two respective host-rocks. The permeabilities of the sandstones that host the Virgin River mineralization and of the crystalline basement rocks that host the McArthur River deposit are similar, and the post-mineralizing fluid flow is mostly fracture-controlled. The Virgin River area has been subject to significantly more fracturing because of the presence of the Dufferin Lake Fault, which is part of the Virgin River crustal shear-zone (Hoeve & Quirt 1984). As a result, enhanced circulation of fluid along structures present at the Virgin River prospect was conducive to a more significant alteration of uraninite.

AGE ESTIMATES BASED ON THE SUBSTITUTIONS

The initial composition of uraninite contains minimal Fe, Si, and Ca. The alteration of uraninite and the increase of these elements are expected to result in a decrease in radiogenic lead. Therefore, the age of formation of the uraninite in the McArthur River deposit can be deciphered by extrapolating the chemical U–Pb ages to the age when the concentrations of the substitution elements (Si, Ca, and Fe) were negligible in the uraninite. If all of the substituting elements are considered as a total, the regression to zero content of these elements corresponds to 1601 ± 63 Ma (Fig. 9A). The intercept for calcium is at 1629 ± 72 Ma (Fig. 9B). Extrapolation for each of the substituting elements does not indicate the same initial age, with the intercept age of iron substitution at 1360 ± 54 Ma for the low-iron group and 1405 ± 48 Ma for the high-iron group (Fig. 9C), and the intercept for silicon at 1425 ± 58 Ma.

The age of *ca.* 1601 Ma estimated from the intercept of the total of all substituting elements and the age of *ca.* 1629 Ma estimated from the intercept of calcium are within analytical uncertainty of the age of 1570 ± 19 Ma obtained by $^{207}\text{Pb}/^{206}\text{Pb}$ dating of the same uraninite

TABLE 3. RESULTS OF ELECTRON-MICROPROBE ANALYSES AND CALCULATED AGE FOR URANINITE FROM THE SEDIMENT-HOSTED VIRGIN RIVER PROSPECT, ATHABASCA BASIN, CANADA

	SiO ₂	PbO	UO ₂	FeO	CaO	TiO ₂	Total	Age
VR03-827 A-1	0.32	0.53	84.67	0.96	1.45	0.21	88.13	42.8
VR03-827 A-2	0.40	0.56	88.28	1.17	1.16	0.20	91.76	46.3
VR03-827 A-3	0.26	0.53	83.30	3.13	1.56	0.30	89.09	44.1
VR03-827 A-4	0.27	0.61	79.04	4.07	1.52	0.23	85.74	53.2
VR03-827 A-5	0.25	0.40	86.23	0.91	1.58	0.25	89.61	31.8
VR03-827 A-6	0.29	0.33	87.22	0.87	1.60	0.27	90.58	25.9
VR03-827 A-7	0.24	0.52	85.66	1.78	1.46	0.25	89.90	41.5
VR03-827 A-8	0.27	0.40	85.51	0.86	1.70	0.26	89.00	32.3
VR03-827 A-9	0.25	0.36	86.09	0.91	1.87	0.26	89.74	28.6
VR03-827 A-10	0.30	0.31	83.59	0.92	1.91	0.24	87.26	25.5
VR03-827 A-11	0.28	0.18	84.82	1.21	1.71	0.24	88.44	14.5
Average	0.28	0.43	84.95	1.53	1.59	0.25		
$\pm 1\sigma$	0.04	0.13	2.44	1.08	0.21	0.03		

The compositions are reported in wt%, and the age, in Ma.

samples and of the $^{40}\text{Ar}/^{39}\text{Ar}$ age of 1591 ± 21 Ma for coeval illite (Alexandre *et al.* 2005). Similarity of the inferred intercept-ages with the ages obtained using more robust isotopic systems suggests that the intercept ages based on substituting elements may be reliable. On the other hand, dating of uraninite using chemical U–Pb ages (Bowles 1990) can lead to inaccurate ages because uraninite is susceptible to lead loss, as our data indicate. Therefore, chemical U–Pb ages should be interpreted in conjunction with the chemical composition of natural samples of uraninite.

The ages of *ca.* 1360 and *ca.* 1405 Ma obtained from the intercept of the low-iron and high-iron substitutions (Fig. 9C) correspond to a time of increased amounts of dissolved iron in the alteration fluids. They are similar to *ca.* 1400 Ma, the U/Pb ages of uraninite

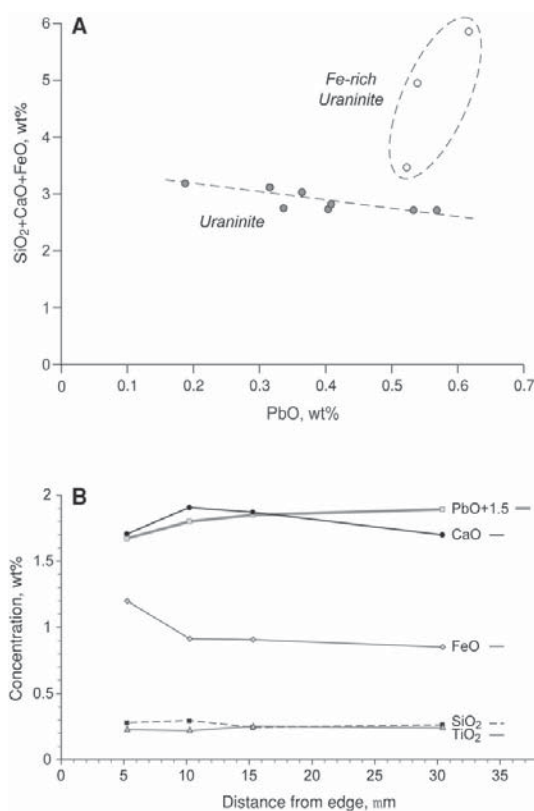


FIG. 7. Compositional variation of uraninite from the sediment-hosted Virgin River prospect. (A) Negative correlation between $\text{SiO}_2 + \text{CaO} + \text{FeO}$ and PbO , with the exception of three points with higher Fe contents. (B) Concentration of various elements as function of the distance to the edge of a grain from the sandstone-hosted Virgin River prospect. The Pb concentration has been shifted by 1.5 wt% in order to permit comparison with the Ca concentration. The grain is shown in Figure 4C.

found throughout the Athabasca Basin (Carl *et al.* 1991, Philippe *et al.* 1993, Baadsgard *et al.* 1984). The difference in substitution-based intercept ages obtained for calcium and for iron indicates that there was a significant change in fluid composition moving along the fracture system with time, as should be expected.

FACTORS CONTROLLING THE SUBSTITUTIONS

The intensity and character of the alteration of uraninite from Virgin River and from McArthur River are a function of the amount and chemical and physical characteristics of the alteration fluids, which in turn depend on the host-rock lithology and structure. Of primary importance is the availability of substituting elements in the alteration fluids, as exemplified by the evolution of the composition of uraninite from the McArthur River deposit, where calcium increases in the fluid at *ca.* 1600 Ma, and iron and silica at *ca.* 1400 Ma. The chemical composition of the fluid is modified by interactions with the host rocks to the uranium mineralization.

Another factor is the capacity of the fluids to oxidize, as uranium silicates tend to form under reducing conditions, whereas various uranyl minerals tend to form under oxidizing conditions (Finch & Murakami 1999). Although later fluids in the basin are most likely oxidizing, interaction with lithologies in the crystalline basement, particularly those with graphite, could render them more reducing and enhance formation of coffinite rather than uranyl phases. Thus, substitutions in uraninite are, at least partly, controlled by the composition of host-rock minerals, which can control the redox state of the fluids.

SUMMARY

In the present study, we illustrate the effects of element substitution in natural uraninite from two different settings, the basement-hosted McArthur River deposit and the sediment-hosted Virgin River prospect

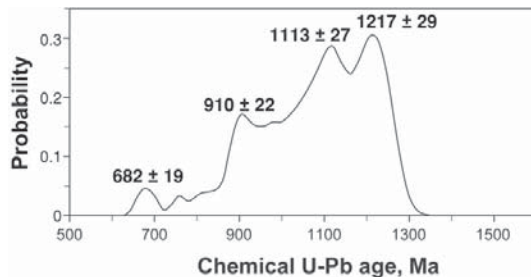


FIG. 8. Cumulative probability diagram of chemical U-Pb ages from the McArthur River deposit, showing the presence of four distinct age-groups. The average ages and the error margins of these groups are indicated.

in the Athabasca Basin. Petrographic observations and SEM images record the effects of alteration and recrystallization of uraninite and the formation of new minerals of uranium, and substantiate the great chemical

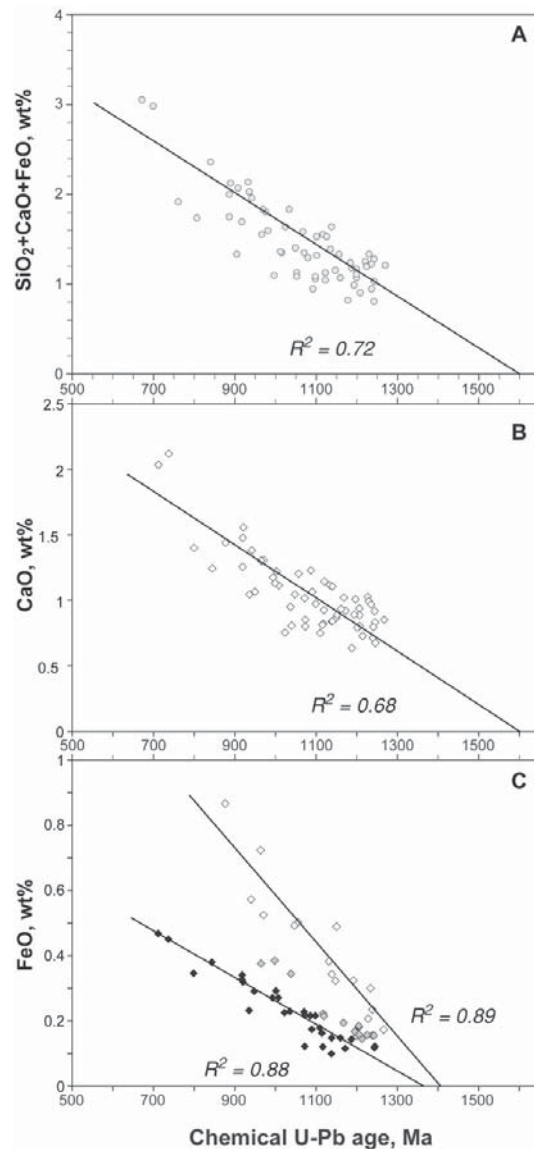


FIG. 9. Variation of the SiO_2 , CaO , and FeO contents of uraninite from the McArthur River deposit as function of the chemical U-Pb age. The linear regression lines of $\text{SiO}_2 + \text{CaO} + \text{FeO}$ (A) and of CaO (B) intercept the age axis at *ca.* 1600 Ma, whereas the regression of FeO (C) intercepts the age axis at *ca.* 1400 Ma, with a small difference between high-iron and low-iron populations. The linear regression coefficients (R^2) are indicated.

heterogeneity of natural uraninite, summarized by Finch & Murakami (1999). The size of the domains with homogeneous chemical composition is variable, but usually less than ten micrometers.

Electron-microprobe analyses indicate that uraninite readily exchanges elements with the later fluids. In particular, radiogenic Pb is replaced by Ca, Si, and Fe (Janeczek & Ewing 1992b) *via* discrete alteration of uraninite. The most significant substitution leads to conversion of uraninite to coffinite, with up to 10 wt% SiO₂. The character of the substitutions depends on the amount and composition of the alteration fluids, particularly their capacity for oxidation. Many of the chemical factors are influenced, to a certain degree, by the characteristics of the host rocks.

Calculated chemical U–Pb ages are much younger than those obtained by isotopic dating, as Pb leaves the uraninite. The chemical U–Pb ages should thus be used with caution, and in all cases, in conjunction with the chemical composition of the uraninite. Regression of the concentrations of the substituting element can indicate initial ages of crystallization in some cases.

ACKNOWLEDGEMENTS

This work benefitted from financial contribution by the Natural Sciences and Engineering Research Council of Canada (NSERC) *via* Discovery, Major Facility Access and Collaborative Research and Development grants. Cameco Corp. is acknowledged for its financial support. Dan Jiricka and Vladimir Sopuck are thanked for their field support and constructive discussions. The authors are grateful to referees R. Tessardi and J. Janeczek, Associate Editor Sergey Krivovichev and Robert F. Martin for constructive and insightful comments, which greatly improved the quality of the manuscript.

REFERENCES

- ALEXANDRE, P., KYSER, T.K. & POLITO, P. (2005): Petrogenesis of Paleoproterozoic basement-hosted unconformity-type uranium deposits in the Athabasca Basin, Canada. *Econ. Geol.* (in press)
- BAADSGAARD, H., CUMMING, G.L. & WORDEN J.M. (1984): U–Pb geochronology of minerals from the Midwest uranium deposit, northern Saskatchewan. *Can. J. Earth Sci.* **21**, 642–648.
- BOWLES, J.F.W. (1990): Age dating of individual grains of uraninite in rocks from electron microprobe analyses. *Chem. Geol.* **83**, 47–53.
- BROOKINS, D.G. (1978): Geochemical genesis of uranium in the southern San Juan Basin. *NURE Uranium Geology Symposium (Grand Junction, 1977), Abstracts and Visual Presentations*, GJBX–12 (78), 67–86.
- BURWASH, R.A., BAADSGAARD, H. & PETERMAN, Z.E. (1962): Precambrian K–Ar dates from the Western Canada sedimentary basin. *J. Geophys. Res.* **67**, 1617–1625.
- CARL, C., VON PECHMANN, E., HÖNDORF, A. & RUHLMANN, G. (1992): Mineralogy and U/Pb, Pb/Pb, and Sm/Nd geochronology of the Key Lake uranium deposit, Athabasca Basin, Saskatchewan, Canada. *Can. J. Earth Sci.* **29**, 879–895.
- FAYEK, M., JANECEK, J. & EWING, R.C. (1997): Mineral chemistry and oxygen isotopic analyses of uraninite, pitchblende and uranium alteration minerals from the Cigar Lake deposit, Saskatchewan, Canada. *Appl. Geochem.* **12**, 549–565.
- _____ & KYSER, T.K. (1997): Characterization of multiple fluid-flow events and rare-earth-element mobility associated with formation of unconformity uranium deposits in the Athabasca Basin, Saskatchewan. *Can. Mineral.* **35**, 627–658.
- _____, _____ & RICIPUTI, L.R. (2002): U and Pb isotope analyses of uranium minerals by ion microprobe and the geochronology of the McArthur River and Sue Zone uranium deposits, Saskatchewan, Canada. *Can. Mineral.* **40**, 1553–1569.
- FINCH, R.J. & EWING, R.C. (1992): The corrosion of uraninite under oxidizing conditions. *J. Nuclear Mater.* **190**, 133–156.
- _____ & MURAKAMI, T. (1999): Systematics and paragenesis of uranium minerals. In *Uranium: Mineralogy, Geochemistry and the Environment* (P.C. Burns & R.J. Finch, eds.). *Rev. Mineral.* **38**, 91–179.
- GRANDSTAFF, D.E. (1976): A kinetic study of the dissolution of uraninite. *Econ. Geol.* **71**, 1493–1506.
- HOEVE, J. & QUIRT, D. (1984): Mineralization and host rock alteration in relation to clay mineral diagenesis and evolution of the middle-Proterozoic Athabasca Basin, northern Saskatchewan, Canada. *Sask. Res. Council, Tech. Rep.* **187**.
- _____ & SIBBALD, T.I.I. (1978): On the genesis of Rabbit Lake and other unconformity-type uranium deposits in northern Saskatchewan, Canada. *Econ. Geol.* **73**, 1450–1473.
- HURÉ, J. & ELSTON, J. (1960): Propriétés de l'uranium combiné et en solution. In *Nouveau Traité de Chimie Minérale. XV. Uranium and Transuraniens* (R. Caillat & J. Elston, eds.). Masson, Paris, France.
- ISOBE, H., MURAKAMI, T. & EWING, R.C. (1992): Alteration of uranium minerals in the Koongara deposit, Australia: unweathered zone. *J. Nucl. Mater.* **190**, 174–187.
- JANECEK, J. & EWING, R.C. (1992a): Structural formula of uraninite. *J. Nucl. Mater.* **190**, 128–132.

- _____ & _____ (1992b): Dissolution and alteration of uraninite under reducing conditions. *J. Nucl. Mater.* **190**, 157-173.
- _____ & _____ (1995): Mechanisms of lead release from uraninite in natural fission reactors in Gabon. *Geochim. Cosmochim. Acta* **59**, 1917-1931.
- KEMPE, U. (2003): Precise electron microprobe age determination in altered uraninite: consequences on the intrusion age and the metallogenic significance of the Kirchberg granite (Erzgebirge, Germany). *Contrib. Mineral. Petrol.* **145**, 107-118.
- KOTZER, T.G. & KYSER, T.K. (1993): O, U, and Pb isotopic and chemical variations in uraninite: implications for determining the temporal and fluid history of ancient terrains. *Am. Mineral.* **78**, 1262-1274.
- KYSER, K., HIATT, E.E., RENAC, C., DUROCHER, K., HOLK, G. & DECKART, K. (2000): Diagenetic fluids in Paleo- and Meso-Proterozoic sedimentary basins and their implications for long protracted fluid histories. In *Fluids and Basin Evolution* (T.K. Kyser, ed.). *Mineral. Assoc. Can., Short Course Vol. 28*, 225-262.
- LECHEMINANT, A.N. & HEAMAN, L.M. (1989): Mackenzie igneous events, Canada: middle Proterozoic hotspot magmatism associated with ocean opening. *Earth Planet. Sci. Lett.* **96**, 38-48.
- LEWRY, J.F. & SIBBALD, T.I.I. (1980): Thermotectonic evolution of the Churchill Province in northern Saskatchewan. *Tectonophysics* **68**, 45-82.
- MCGILL, B.D., MARLAT, J.L., MATTHEWS, R.B., SOPUCK, V.J., HOMENIUK, L.A. & HUBREGTSE, J.J. (1993): The P2 North uranium deposit, Saskatchewan, Canada. *Explor. Mining Geol.* **2**, 321-331.
- MEDARIS, L.G., SINGER, B.S., DOTT, R.H., NAYMARK, A., JOHNSON, C.M. & SCHOTT, R.C. (2003): Late Paleoproterozoic climate, tectonics, and metamorphism in the southern Lake Superior region and proto-North America; evidence from Baraboo interval quartzites. *J. Geol.* **111**, 243-257.
- MOORE, J.M. (1986): Introduction: the "Grenville Problem" then and now. In *The Grenville Province* (J.M. Moore, A. Davidson, & A.J. Baer, eds.). *Geol. Assoc. Can., Spec. Pap.* **31**, 1-11.
- PHILIPPE, S., LANCELOT, J.R., CLAUER, N. & PAQUET, A. (1993): Formation and evolution of the Cigar Lake uranium deposit based on U-Pb and K-Ar isotope systematics. *Can. J. Earth Sci.* **30**, 720-730.
- RAMAEKERS, P. (1990): Geology of the Athabasca Group (Helikian) in northern Saskatchewan. *Saskatchewan Energy and Mines, Saskatchewan Geol. Surv., Rep.* **195**.
- RANCHIN, G. (1968): Contribution à l'étude de la répartition de l'uranium à l'état de traces dans les roches granitiques saines: les uraninites à teneur élevée du Massif de Saint-Sylvestre (Limousin, Massif Central français). *Sciences de la Terre* **13**, 159-198.
- ROMANO, D., HOLM, D.K. & FOLAND, K.A. (2000): Determining the extent and nature of Mazatzal-related overprinting of the Penokean Orogenic belt in the southern Lake Superior region, north-central USA. *Precamb. Res.* **104**, 25-46.
- SIBBALD, T.I.I. & QUIRT, D. (1987): Uranium deposits of the Athabasca Basin. *Geol. Assoc. Can. - Mineral. Assoc. Can., Field Trip Guidebook, Trip 9*. *Saskatchewan Res. Council, Publ.* **R-855-1-G-87**.

Received July 23, 2004, revised manuscript accepted February 19, 2005.